

PathCoT: Chain-of-Thought Prompting for Zero-shot Pathology Visual Reasoning

Junjie Zhou^{1,2}, Yingli Zuo^{1,2}, Shichang Feng^{1,2}, Peng Wan^{1,2}, Qi Zhu^{1,2},
Daoqiang Zhang^{1,2*}, and Wei Shao^{1,2*}

¹ The College of Artificial Intelligence, Nanjing University of Aeronautics and Astronautics

² The Key Laboratory of Brain-Machine Intelligence Technology, Ministry of Education

Abstract. With the development of generative artificial intelligence and instruction tuning techniques, multimodal large language models (MLLMs) have made impressive progress on general reasoning tasks. Benefiting from the chain-of-thought (CoT) methodology, MLLMs can solve the visual reasoning problem step-by-step. However, existing MLLMs still face significant challenges when applied to pathology visual reasoning tasks: (1) LLMs often underperforms because they lack domain-specific information, which can lead to model hallucinations. (2) The additional reasoning steps in CoT may introduce errors, leading to the divergence of answers. To address these limitations, we propose PathCoT, a novel zero-shot CoT prompting method which integrates the pathology expert-knowledge into the reasoning process of MLLMs and incorporates self-evaluation to mitigate divergence of answers. Specifically, PathCoT guides the MLLM with prior knowledge to perform as pathology experts, and provides comprehensive analysis of the image with their domain-specific knowledge. By incorporating the experts' knowledge, PathCoT can obtain the answers with CoT reasoning. Furthermore, PathCoT incorporates a self-evaluation step that assesses both the results generated directly by MLLMs and those derived through CoT, finally determining the reliable answer. The experimental results on the PathMMU dataset demonstrate the effectiveness of our method on pathology visual understanding and reasoning.

Keywords: Pathology visual reasoning · Chain-of-thought · Multimodal.

1 Introduction

In recent years, the development of generative artificial intelligence has led to the emergence of multimodal large language models (MLLMs), which are capable of processing multimodal inputs, such as images and text, by aligning visual representations with the input space of large language models (LLMs) [1–4]. Facilitated by instruction tuning, models like LLaVa [2] and GPT-4V [5] have

* Corresponding authors.

showcased advanced capabilities in human interaction and reasoning, which enables MLLMs to follow human instructions and complete real-world tasks. These advancements have fueled enthusiasm within the AI community, leading to the emergence of MLLMs in medical fields, including radiology [6, 7] and pathology [8–10], where they hold promise for advancing diagnostic support and complex reasoning.

Chain-of-Thought (CoT) methods have emerged as a powerful tool to enhance the reasoning capabilities of LLMs, achieving notable success in natural language processing (NLP) [11–13]. It follows a divide-and-conquer approach, breaking down complex problems into multi-step reasoning tasks. Recently, several studies have extended CoT to MLLMs, significantly boosting their reasoning abilities [14–17]. For instance, MM-CoT [14] first proposes a two-stage framework on complex reasoning tasks with language and vision modalities by separating rationale generation and answer inference. CCoT [18] generates the scene graph (SG) to describe the visual scene, and then integrates it as the prompt to produce a response for multimodal and compositional visual reasoning. CoCoT [17] focuses on multiple image inputs that can prompt LMMs to discern and articulate the similarities and differences among inputs, laying the groundwork for answering multi-image-based questions.

Although much progress has been achieved for general visual reasoning tasks, MLLMs still face significant challenges when applied to pathology visual reasoning tasks:

1. Existing MLLMs underperform on pathology visual reasoning tasks due to the lack of domain-specific knowledge. For instance, the recent work [19] curates a multimodal dataset PathMMU for understanding and reasoning in pathology, and find it that current MLLMs still struggle with the PathMMU. Even the most advanced models exhibit a significant performance gap compared to professional pathologists [19]. This is primarily because current LLMs are trained on general-domain data that may generate incorrect answers or even hallucinations when working on specialized pathology reasoning tasks. One potential solution is to fine-tune models on specialized pathology datasets. However, the traditional fine-tuning paradigm not only requires the collection of domain-specific data but also consumes substantial computational resources, which has limitations in scalability.

2. The additional reasoning steps in CoT may introduce errors, leading to divergence of answers. We find that the intermediate reasoning steps in CoT reasoning may introduce additional incorrect knowledge due to model hallucinations (see Fig. 2). This causes the divergence of results between the answers derived by CoT and those from direct reasoning, and in some cases, the CoT-based results may even be worse than the direct reasoning results (see Tab. 1). This divergence of answers in pathology reasoning can lead to serious consequences, such as misdiagnoses, inappropriate treatments, or delays in critical interventions [20]. Consequently, it is essential to re-evaluate CoT-based results for assessing their reliability.

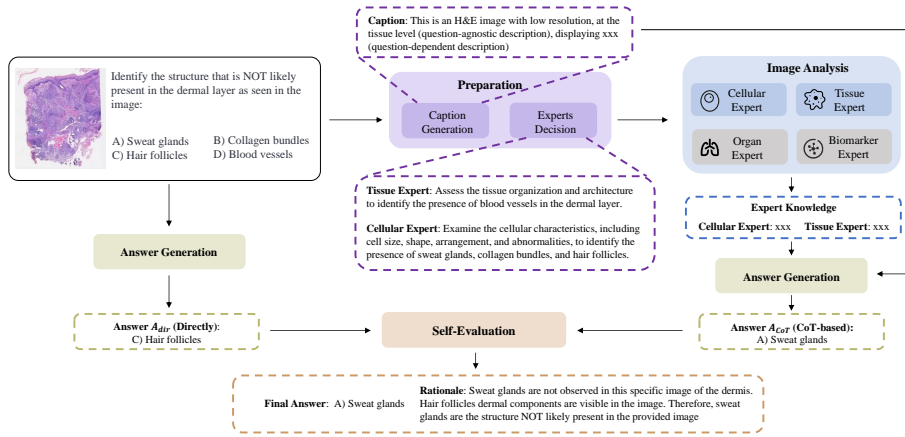


Fig. 1. The framework of our proposed PathCoT.

To address the above limitations, we propose PathCoT, a novel CoT prompting method for zero-shot pathology visual reasoning without any fine-tuning. Specifically, PathCoT firstly generates the pathology image caption which incorporates question-agnostic and question-dependent descriptions. For better analysis of pathology images, PathCoT introduces four pathology experts: Cellular Expert, Tissue Expert, Organ Expert and Biomarker Expert. These experts can provide comprehensive analysis of pathology images with their domain-specific knowledge. By the combination of image caption and experts knowledge, PathCoT can derive the answer with CoT reasoning. Finally, PathCoT performs a self-evaluation process that considers both the results directly generated by MLLMs and those derived through CoT for the determination of the final answer. We conduct experiments on the PathMMU dataset [19], which is a massive multimodal expert-level benchmark for understanding and reasoning in pathology. The experimental results demonstrate the effectiveness of our method on pathology visual understanding and reasoning.

2 Method

2.1 Overview

Given the question Q and image I , PathCoT aims to generate their corresponding answer. The input of PathCoT consists of two modalities: text and image. In addition to the question Q , the text modality also includes supplementary information, such as captions, expert-knowledge, etc. The overall framework of PathCoT is shown in Fig. 1. The framework consists of four stages: Preparation (Sec. 2.2), Image Analysis (Sec. 2.3), Summary & Answer Generation (Sec. 2.4) and Self-Evaluation (Sec. 2.5).

2.2 Preparation

PathCoT initially prepares for CoT reasoning, consisting of two tasks: caption generation and expert decision. Specifically, the caption generation task identifies descriptive pathological features, while the expert decision task determines the appropriate experts for subsequent image analysis. Previous studies [15, 21] demonstrate that the descriptive information can help MLLMs better understand the image and accurately answer the question. Therefore, PathCoT generates the image caption, denoted as D_{cap} , which contains descriptive information of the pathology image. Particularly, we consider two types of descriptions in D_{cap} : question-agnostic description D_{qa} and question-dependent description D_{qd} . Thus, the image caption D_{cap} can be formulated as: $D_{cap} = \{D_{qa}, D_{qd}\}$.

Question-agnostic description D_{qa} is independent of the question Q , and contains basic information about the pathology image, such as image type, field of view, etc. Specifically, we can prompt the MLLMs with the following instructions: *Identify the type of pathology image (e.g., HE, IHC, Gross Pathology, etc), assess the image quality (e.g., resolution, clarity, and any noise), and specify the scope of observation (cellular, tissue, or organ level).*

On the other hand, the question-dependent description D_{qd} focuses on identifying pathological image features that may be relevant to the given question Q . For instance, if the question is related to the presence of tumor cells in the image, the question-dependent description would focus on identifying abnormal cell morphology, mitotic activity, and staining patterns indicative of malignancy. The following prompt can be used to generate D_{qd} : *Describe the key features of the image that are relevant to the question. Initial observations should focus on identifying the primary components, staining patterns, and any notable abnormalities visible within the provided field.*

Additionally, PathCoT prepares for determining appropriate experts based on the given question for subsequent analysis. Specifically, PathCoT firstly identifies each expert and its corresponding responsibility (detailed in Sec. 2.3). Then, by taking the image, question and experts’ responsibilities as input, PathCoT generates the decision information, denoted as I_{dec} . This decision information contains the selection and guidance results, where the selection results indicate whether the given question can be addressed using the knowledge of the corresponding expert and the guidance I_G provides instructions on how to leverage the selected experts to analyze the image. This guidance is subsequently used to direct the MLLM in generating the corresponding expert-knowledge.

2.3 Image Analysis

Pathology visual reasoning requires a comprehensive analysis of pathology images, encompassing various biological levels—from individual cells to entire organs, as well as the mechanisms related to biomarkers. To effectively address pathology-related visual reasoning tasks and enhance the analysis of pathology images, PathCoT introduces the following four experts: **Cellular Expert** analyzes cellular characteristics, including cell size, shape, arrangement, and abnormalities. **Tissue Expert** focuses on the organization and architecture of tissue,

examining the spatial relationships between components like epithelium, stroma, and blood vessels. **Organ Expert** specializes in the analysis of organ-level structures, assessing the overall anatomical integrity and functional zones of the organ. **Biomarker Expert** is responsible for identifying crucial biomarkers for diagnosis, prognosis, and understanding disease mechanisms. These experts are designed to capture distinct yet complementary pathological features. By the combination of the mentioned experts’ knowledge, we obtain $E = \{E_C, E_T, E_O, E_B\}$ to analyze images, where E_C, E_T, E_O, E_B represent the expert-knowledge from the Cellular, Tissue, Organ, and Biomarker Experts, respectively. Each expert’s knowledge is generated by the MLLM with the guidance I_G in the decision information I_{dec} .

Inspired by Mixture of Experts (MoE) [22] that not all experts are required for image analysis, we select related experts based on specific questions (as discussed in Sec. 2.2). Only the selected experts analyze the image, and their insights are aggregated and synthesized to form the final expert-knowledge E .

2.4 Summary & Answer Generation

Once the preparation and analysis stages are completed, PathCoT summarizes all acquired information including Image I , Question Q , image caption D_{cap} and expert-knowledge E as $S = \{I, Q, D_{cap}, E\}$. Finally, PathCoT generates the CoT-based answer A_{CoT} as follows:

$$A_{CoT} = MLLM(S). \quad (1)$$

2.5 Self-Evaluation

To improve the reliability of results, PathCoT re-evaluates CoT-based answers since the additional reasoning steps in CoT may introduce errors. These errors may cause the CoT-based answers to be less accurate than the direct reasoning answers, leading to the divergence of answers. To address such divergence, PathCoT performs a self-evaluation stage that assesses the generated answers. In addition to the answer A_{CoT} generated by CoT, we obtain another direct reasoning answer A_{dir} generated by the MLLM without the CoT reasoning process:

$$A_{dir} = MLLM(I, Q). \quad (2)$$

Then, PathCoT considers both answers as candidates and determines the correct one (as shown in Fig. 1). When faced with conflicting candidate answers, PathCoT should provide the additional rationale R for the decision, including the justification for selecting the correct answer and the explanation for rejecting the incorrect answer. Therefore, the final answer A can be obtained by:

$$R, A = MLLM(I, Q, A_{CoT}, A_{dir}). \quad (3)$$

Table 1. Performance comparisons of different methods on the PathMMU dataset.

Method	PubMed		EduContent		Atlas		PathCLS		Overall	
	Tiny Test (281)	Test (2787)	Tiny Test (255)	Test (1683)	Tiny Test (208)	Test (799)	Tiny Test (177)	Test (1632)	Tiny Test (921)	Test (6901)
MLLM Only	39.15	36.35	33.33	35.59	37.02	34.79	21.47	19.98	33.66	32.11
MMCoT	40.93	35.24	30.59	36.07	33.65	32.79	20.90	21.63	32.57	31.94
DDCoT	31.67	31.40	28.63	32.20	31.73	31.54	18.08	17.77	28.23	28.39
Cantor	38.08	34.09	36.86	33.21	37.50	34.92	18.64	18.32	33.88	30.24
CCoT	41.64	35.13	32.16	34.82	34.62	33.42	22.03	22.06	33.66	31.76
Qvix	35.23	32.62	34.90	34.88	34.62	33.79	21.47	18.44	32.36	29.95
MC-CoT	39.86	36.96	35.29	36.19	38.46	35.29	19.77	21.20	34.42	32.85
PathCoT	45.55	40.90	39.22	40.17	42.79	42.43	24.86	23.44	39.20	36.75

Table 2. Ablation studies for each stage in PathCoT.

Method	PubMed		EduContent		Atlas		PathCLS		Overall	
	Tiny Test	Test								
w/o Caption	44.13	39.76	36.86	38.27	40.38	40.55	23.16	22.79	37.24	35.47
w/ Vanilla Caption	44.84	40.04	37.65	39.28	41.35	41.43	23.73	22.98	38.00	35.98
w/o Analysis	42.35	38.75	34.51	36.84	38.46	38.92	22.60	21.38	35.50	34.20
w/o Self-Evaluation	43.06	39.22	37.25	37.97	39.42	40.43	23.16	22.67	36.81	35.14
PathCoT	45.55	40.90	39.22	40.17	42.79	42.43	24.86	23.44	39.20	36.75

3 Experiments

3.1 Dataset and Settings

We evaluate the performance of PathCoT on the PathMMU dataset [19], a massive multimodal expert-level benchmark for understanding and reasoning in pathology. It includes 33,573 Q&As along with 21,599 pathology images. We conduct our experiments on four subsets of PathMMU: PubMed, SocialPath, Atlas, and PathCLS. Each subset contains two test data: the tiny test set and test set, we evaluate our method on both of them.

PathCoT is implemented using PyTorch [23] on a single GPU (NVIDIA GeForce RTX 3090). We use LLava as the MLLM in PathCoT. For fair comparison, all comparison methods also utilize LLaVa as the MLLM. GPT-3.5 is employed as the language tool if an LLM is required.

3.2 Baselines and Metric

To demonstrate the effectiveness of PathCoT, we compare it with state-of-the-art (SOTA) zero-shot CoT-based methods as follows: **MLLM-Only**: directly applies the MLLM model to answer the question based on the image. **MM-CoT** [14]: generates rationales based on ground truth before producing the final answer. **DDCoT** [16]: uses the LLM to break down the problem into multiple related sub-questions and then answers each sub-questions. **CCoT** [18]: obtains scene graphs and integrates it as the prompt for visual reasoning. **Cantor** [24]: utilizes the advanced cognitive abilities of the MLLM for general high-level logical problem-solving. **Qvix** [15]: applies MLLM to explore visual information

Table 3. Ablation studies for each expert in PathCoT.

Method	PubMed		EduContent		Atlas		PathCLS		Overall	
	Tiny	Test								
w/o Cellular Expert	43.42	39.40	36.08	38.15	39.90	40.30	23.16	22.55	36.70	35.21
w/o Tissue Expert	43.77	39.54	36.47	38.32	40.38	40.80	23.16	22.37	37.02	35.33
w/o Organ Expert	44.84	40.11	37.65	39.22	41.38	41.80	24.29	23.10	38.11	36.07
w/o Biomarker Expert	44.13	39.94	37.25	38.80	40.87	41.55	23.73	22.86	37.57	35.81
PathCoT	45.55	40.90	39.22	40.17	42.79	42.43	24.86	23.44	39.20	36.75

based on the knowledge derived from LLMs. **MC-CoT** [21]: designs a modular collaborative CoT framework for med-vqa tasks by integrating LLMs into the problem-solving process. We evaluate our method by the index of Accuracy since all the questions in the test sets are in the form of multiple-choice questions.

3.3 Comparisons with SOTA CoT-based methods

In Tab. 1, we compare our method with other zero-shot CoT-based methods on the PathMMU dataset. From Tab. 1, we can draw the following observations: Firstly, these general CoT-based methods, which are not specifically designed for pathology images, perform poorly on pathology visual reasoning tasks due to the lack of domain-specific information, resulting in lower accuracy than results generated directly by MLLMs. Secondly, both MC-CoT and PathCoT introduce specific module to handle pathology images, and achieve better performance. Finally, PathCoT consistently outperforms all comparison methods as it takes into account both expert-knowledge and divergence of answers during reasoning.

3.4 Ablation Study

Impact of different stages. We conduct the experiments to verify the effectiveness of different stages in PathCoT, and summarize the results in Tab 2. For ablating the Preparation stage, we establish two baselines: one without the caption (“w/o Caption”) and one with the vanilla caption (“w/ Vanilla Caption”). The “w/o Caption” baseline predicts the answers without generating captions, while the “w/ Vanilla Caption” baseline directly generates captions without considering the question-agnostic and question-dependent descriptions. From the first two rows of the Tab. 2, we can observe that both the vanilla caption and our designed caption can improve the reasoning accuracy. Furthermore, our designed caption can lead to an increase of 1.20% and 0.77% on the overall tiny test and test sets, respectively, compared to the vanilla caption baseline. These results demonstrate the importance of question-agnostic and question-dependent descriptions in helping MLLMs better understand the image and answer the given questions more accurately. In addition, the analysis stage improves the results by 3.70% and 2.55% on the overall tiny test and test sets, respectively, as shown in the third row of Tab. 2. This improvement is driven by the integration of knowledge from different experts in analyzing pathology images, which benefits visual reasoning tasks. Finally, results are improved by 2.39% and 1.61%

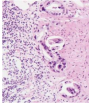
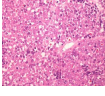
Case 1	Case 2
 <p>Regarding the stroma in this image, what is the predominant cellular infiltration observed?</p> <p>A) Muscle fibers with elongated nuclei B) Fibroblasts with spindle-shaped nuclei C) Adipocytes with large clear cytoplasm D) Inflammatory cells with densely stained nuclei</p>	 <p>What can be inferred about the cellular arrangement and cytoplasm of the cells in this tissue sample?</p> <p>A) Spindle-shaped cells with abundant eosinophilic cytoplasm B) Cells with abundant cytoplasm forming acinar structures C) Cells with clear cytoplasm arranged in sheets D) Small to medium-sized cells with scant cytoplasm and irregular outlines</p>
<p>Directly</p> <p>Answer: B) Fibroblasts with spindle-shaped nuclei ❌</p>	<p>Directly</p> <p>Answer: D) Small to medium-sized cells with scant cytoplasm and irregular outlines ✅</p>
<p>CoT-based</p> <p>Answer: D) Inflammatory cells with densely stained nuclei</p> <p>Tissue Expert: The image displays a close-up view of a tissue sample, likely from the breast, with a focus on the organization and architecture of the tissue. The stroma is visible in the background, and the blood vessels are scattered throughout the tissue. There are several blood vessels of different sizes and shapes, with some appearing to be dilated or congested. The tissue also exhibits some signs of inflammation, as evidenced by the presence of inflammatory cells. ✅</p>	<p>CoT-based</p> <p>Answer: A) Spindle-shaped cells with abundant eosinophilic cytoplasm</p> <p>Cellular Expert: The image displays a close-up view of a pink cellular structure, possibly a blood cell or a tissue sample. The cellular arrangement consists of numerous small red dots, which are likely the cell's cytoplasm. These dots are scattered throughout the cellular structure, creating a visually striking pattern. The presence of these dots suggests that the cell is actively engaged in various cellular processes, such as metabolism or communication. ❌</p>
<p>Self-Evaluation</p> <p>Final Answer: D) Inflammatory cells with densely stained nuclei</p> <p>Rationale: Upon examining the image, the predominant cellular infiltration in the stroma appears to consist of numerous cells with densely stained nuclei. These are indicative of inflammatory cells, such as lymphocytes or other types of white blood cells, which typically infiltrate tissues as part of an inflammatory response. In contrast, fibroblasts tend to have elongated and spindle-shaped nuclei, but they do not appear as densely packed and darkly stained present in this image. Therefore, answer D is consistent with the observed morphological features in the image, whereas B is not. ✅</p>	<p>Self-Evaluation</p> <p>Final Answer: D) Small to medium-sized cells with scant cytoplasm and irregular outlines</p> <p>Rationale: Upon examining the provided histology image, the tissue sample shows a dense arrangement of small to medium-sized cells with relatively high nuclear-to-cytoplasmic ratios, suggesting scant cytoplasm. Many cells also display irregular outlines, which supports candidate answer D. In contrast, spindle-shaped, eosinophilic cells are not evident in the image provided. Therefore, the evidence from the image aligns more closely with candidate answer D. ✅</p>

Fig. 2. The cases of PathCoT.

with the self-evaluation stage (fourth row of Tab. 2). This demonstrates that the proposed self-evaluation process can effectively address divergence of answers and improves the overall accuracy of the results.

Impact of different experts. To highlight the importance of each expert in PathCoT, we present the results in Tab. 3 when specific expert is excluded. The results indicate that each expert contributes positively to PathCoT. Moreover, we observe that the Cellular and Tissue experts are more effective than other experts, implying their crucial role in pathology visual reasoning tasks.

3.5 Case Presentation

In this section, we provide two cases to demonstrate how PathCoT effectively utilizes reasoning chains to derive correct results, as shown in Fig. 2.

In Case 1, we present how expert-knowledge can significantly aid the reasoning process by providing valuable information. For instance, the Tissue Expert provides the knowledge: *The tissue also exhibits some signs of inflammation, as evidenced by the presence of inflammatory cells*, which helps the MLLM perform reliable reasoning and obtain the right answer.

In Case 2, we show how self-evaluation addresses the divergence of answers. As shown in Fig. 2, the knowledge from the Cellular Expert: *The cellular arrangement consists of numerous small red dots, which are likely the cell's cytoplasm*, introduces error information, and finally results in incorrect answer. However, MLLM is able to predict the right answer by direct reasoning. In face with the divergent answers, PathCoT performs the self-evaluation that can choose the right answer and provide rationales for the decision.

4 Conclusion

We propose PathCoT, a novel CoT prompting method for zero-shot pathology visual reasoning, which integrates the pathology expert-knowledge into the reasoning process of MLLMs and incorporates self-evaluation to mitigate divergence of answers in CoT reasoning. The experimental results verify the efficacy of our method on pathology visual understanding and reasoning.

References

1. Junnan Li, Dongxu Li, Silvio Savarese, and Steven Hoi. Blip-2: Bootstrapping language-image pre-training with frozen image encoders and large language models. In *International conference on machine learning*, pages 19730–19742. PMLR, 2023.
2. Haotian Liu, Chunyuan Li, Qingyang Wu, and Yong Jae Lee. Visual instruction tuning. *Advances in neural information processing systems*, 36, 2024.
3. Wenliang Dai, Junnan Li, Dongxu Li, Anthony Meng Huat Tiong, Junqi Zhao, Weisheng Wang, Boyang Li, Pascale Fung, and Steven Hoi. Instructblip: Towards general-purpose vision-language models with instruction tuning. *arXiv preprint arXiv:2305.06500*, 2023.
4. Deyao Zhu, Jun Chen, Xiaoqian Shen, Xiang Li, and Mohamed Elhoseiny. Minigt-4: Enhancing vision-language understanding with advanced large language models. *arXiv preprint arXiv:2304.10592*, 2023.
5. Josh Achiam, Steven Adler, Sandhini Agarwal, Lama Ahmad, Ilge Akkaya, Florencia Leoni Aleman, Diogo Almeida, Janko Altschmidt, Sam Altman, Shyamal Anadkat, et al. Gpt-4 technical report. *arXiv preprint arXiv:2303.08774*, 2023.
6. Xuechen Guo, Wenhao Chai, Shi-Yan Li, and Gaoang Wang. Llava-ultra: Large chinese language and vision assistant for ultrasound. In *Proceedings of the 32nd ACM International Conference on Multimedia*, pages 8845–8854, 2024.
7. Sewoo Lee, Jiwon Youn, Hyungjin Kim, Mansu Kim, and Soon Ho Yoon. Cxr-llava: a multimodal large language model for interpreting chest x-ray images. *European Radiology*, pages 1–13, 2025.
8. Yuxuan Sun, Chenglu Zhu, Sunyi Zheng, Kai Zhang, Lin Sun, Zhongyi Shui, Yunlong Zhang, Honglin Li, and Lin Yang. Pathasst: A generative foundation ai assistant towards artificial general intelligence of pathology. In *Proceedings of the AAAI Conference on Artificial Intelligence*, volume 38, pages 5034–5042, 2024.
9. Mehmet Saygin Seyfioglu, Wisdom O Ikezogwo, Fatemeh Ghezloo, Ranjay Krishna, and Linda Shapiro. Quilt-llava: Visual instruction tuning by extracting localized narratives from open-source histopathology videos. In *Proceedings of the IEEE/CVF Conference on Computer Vision and Pattern Recognition*, pages 13183–13192, 2024.
10. Ming Y Lu, Bowen Chen, Drew FK Williamson, Richard J Chen, Melissa Zhao, Aaron K Chow, Kenji Ikemura, Ahrong Kim, Dimitra Pouli, Ankush Patel, et al. A multimodal generative ai copilot for human pathology. *Nature*, 634(8033):466–473, 2024.
11. Takeshi Kojima, Shixiang Shane Gu, Machel Reid, Yutaka Matsuo, and Yusuke Iwasawa. Large language models are zero-shot reasoners. *Advances in neural information processing systems*, 35:22199–22213, 2022.

12. Jason Wei, Xuezhi Wang, Dale Schuurmans, Maarten Bosma, Fei Xia, Ed Chi, Quoc V Le, Denny Zhou, et al. Chain-of-thought prompting elicits reasoning in large language models. *Advances in neural information processing systems*, 35:24824–24837, 2022.
13. Zhuosheng Zhang, Aston Zhang, Mu Li, and Alex Smola. Automatic chain of thought prompting in large language models. *arXiv preprint arXiv:2210.03493*, 2022.
14. Zhuosheng Zhang, Aston Zhang, Mu Li, Hai Zhao, George Karypis, and Alex Smola. Multimodal chain-of-thought reasoning in language models. *arXiv preprint arXiv:2302.00923*, 2023.
15. Kaiwen Yang, Tao Shen, Xinmei Tian, Xiubo Geng, Chongyang Tao, Dacheng Tao, and Tianyi Zhou. Good questions help zero-shot image reasoning. *arXiv preprint arXiv:2312.01598*, 2023.
16. Ge Zheng, Bin Yang, Jiajin Tang, Hong-Yu Zhou, and Sibeil Yang. Ddcot: Duty-distinct chain-of-thought prompting for multimodal reasoning in language models. *Advances in Neural Information Processing Systems*, 36:5168–5191, 2023.
17. Daoan Zhang, Junming Yang, Hanjia Lyu, Zijian Jin, Yuan Yao, Mingkai Chen, and Jiebo Luo. Cocot: Contrastive chain-of-thought prompting for large multimodal models with multiple image inputs. *arXiv preprint arXiv:2401.02582*, 2024.
18. Chancharik Mitra, Brandon Huang, Trevor Darrell, and Roei Herzig. Compositional chain-of-thought prompting for large multimodal models. In *Proceedings of the IEEE/CVF Conference on Computer Vision and Pattern Recognition*, pages 14420–14431, 2024.
19. Yuxuan Sun, Hao Wu, Chenglu Zhu, Sunyi Zheng, Qizi Chen, Kai Zhang, Yunlong Zhang, Dan Wan, Xiaoxiao Lan, Mengyue Zheng, et al. Pathmmu: A massive multimodal expert-level benchmark for understanding and reasoning in pathology. In *European Conference on Computer Vision*, pages 56–73. Springer, 2024.
20. Peng Xia, Ze Chen, Juanxi Tian, Yangrui Gong, Ruibo Hou, Yue Xu, Zhenbang Wu, Zhiyuan Fan, Yiyang Zhou, Kangyu Zhu, et al. Cares: A comprehensive benchmark of trustworthiness in medical vision language models. *Advances in Neural Information Processing Systems*, 37:140334–140365, 2025.
21. Lai Wei, Wenkai Wang, Xiaoyu Shen, Yu Xie, Zhihao Fan, Xiaojin Zhang, Zhongyu Wei, and Wei Chen. Mc-cot: A modular collaborative cot framework for zero-shot medical-vqa with llm and mllm integration. *arXiv preprint arXiv:2410.04521*, 2024.
22. Weilin Cai, Juyong Jiang, Fan Wang, Jing Tang, Sunghun Kim, and Jiayi Huang. A survey on mixture of experts. *arXiv preprint arXiv:2407.06204*, 2024.
23. Adam Paszke, Sam Gross, Francisco Massa, Adam Lerer, James Bradbury, Gregory Chanan, Trevor Killeen, Zeming Lin, Natalia Gimelshein, Luca Antiga, et al. Pytorch: An imperative style, high-performance deep learning library. *Advances in neural information processing systems*, 32, 2019.
24. Timin Gao, Peixian Chen, Mengdan Zhang, Chaoyou Fu, Yunhang Shen, Yan Zhang, Shengchuan Zhang, Xiawu Zheng, Xing Sun, Liujuan Cao, et al. Cantor: Inspiring multimodal chain-of-thought of mllm. In *Proceedings of the 32nd ACM International Conference on Multimedia*, pages 9096–9105, 2024.